Bone 125 (2019) 151–159

Contents lists available at ScienceDirect

Bone

journal homepage: www.elsevier.com/locate/bone

Full Length Article

Conditioning of myoblast secretome using mesenchymal stem/stromal cell spheroids improves bone repair

Augustine M. Saiz Jr[a,b,1], Marissa A. Gionet-Gonzales[a,1], Mark A. Lee[b], J. Kent Leach[a,b,*]

[a] Department of Biomedical Engineering, University of California at Davis, Davis, CA 95616, United States of America
[b] Department of Orthopaedic Surgery, UC Davis Health, Sacramento, CA 95817, United States of America

ARTICLE INFO

Keywords:
Muscle
Bone
Secretome
Myokines
Mesenchymal stem/stromal cell

ABSTRACT

Local muscle loss associated with open fractures remains an obstacle to functional recovery and bone healing. Muscle cells secrete bioactive myokines that elicit autocrine and paracrine effects and initiate signaling pathways for regenerating damaged muscle and bone. Mesenchymal stem/stromal cells (MSCs) are under investigation for the regeneration of both muscle and bone through their potent secretome. Compared to monodisperse cells, MSC spheroids exhibit a more complex secretome with heightened therapeutic potential. We hypothesized that the osteogenic potential of myokines would be enhanced when myoblasts were exposed to the MSC spheroid secretome. Conditioned media from MSC spheroids increased osteogenic response of MC3T3 preosteoblasts compared to myokines from L6 myoblasts alone. This effect was synergistically enhanced when conditioned media of MSC spheroids was serially delivered to myoblasts and then osteoprogenitor cells *in vitro*. We then delivered myoblast-stimulated conditioned media in the presence or absence of syngeneic rat bone marrow stromal cells (rBMSCs) from alginate hydrogels to a rat critical-sized segmental defect. We observed increased bone formation in defects treated with conditioned media compared to rBMSCs alone, while bone formation was greatest in defects treated with both conditioned media and rBMSCs over 12 weeks. This foundational study demonstrates a novel approach for capitalizing on the paracrine signaling of muscle cells to promote bone repair and provides additional evidence of the synergistic interaction between muscle and bone.

1. Introduction

Open fractures create major local damage to bone, muscle and skin and are associated with increases in delayed union, nonunion, rehospitalization, infection, revision surgery and worse functional outcomes compared to closed fractures [1]. Successful bone healing is unusual in the presence of an overlying large volume muscle defect, even when stimulated by potent osteoinductive cues such as bone morphogenetic proteins [2]. Even short-term muscle atrophy, modeled by local injection of botulinum toxin, impairs fracture healing in rodents [3]. Autologous vascularized free muscle transplantation remains the gold standard treatment of large volumetric muscle loss injuries when bone is left uncovered by tissue. While this approach can improve fracture healing, it is associated with short- and long-term functional deficits, donor site morbidity, and potential limb loss [4,5]. Cellular therapies, including injection of satellite cells, myogenic progenitor cells, and mesenchymal stem/stromal cells (MSCs) are promising strategies but are plagued by limitations including low viability and poor integration into damaged muscle [6]. While muscle contributes necessary mechanical loading and enables locomotion, it also acts as an endocrine organ, secreting myokines that promote osteogenesis and stimulate surrounding cells in adjacent muscle and bone [7]. Interleukin-8 (IL-8) stimulates angiogenesis, transforming growth factor-β (TGF-β) is a mitogen for osteoblasts, insulin-like growth factor-1 (IGF-1) stimulates bone growth, and matrix metalloproteinase-2 (MMP-2) enables tissue remodeling [7]. Thus, new strategies that mimic the endocrine and paracrine signaling activities of muscle may provide an opportunity to stimulate bone repair.

MSCs from multiple tissue compartments enhance bone healing in various bone models [8,9]. Furthermore, bone marrow aspirate, a rich source of MSCs, promotes the repair of slow or non-healing fractures [10]. However, despite their multilineage potential *in vitro*, there is limited evidence that transplanted MSCs differentiate into osteoblasts *in situ* and directly form bone. Instead, MSCs may have a greater

* Corresponding author at: University of California, Davis, Department of Biomedical Engineering, 451 Health Sciences Dr., Davis, CA 95616, United States of America.
E-mail address: jkleach@ucdavis.edu (J.K. Leach).
[1] These authors contributed equally.

https://doi.org/10.1016/j.bone.2019.05.018
Received 7 February 2019; Received in revised form 4 May 2019; Accepted 14 May 2019
Available online 16 May 2019

therapeutic effect *in vivo via* their potent secretome containing bioactive factors that stimulate angiogenesis, prolong cell viability, induce cell migration, and modulate the local inflammatory environment [11]. For example, MSC transplantation into damaged muscle promoted muscle repair indirectly *via* the secretome instead of direct differentiation into new muscle cells [12].

As an alternative to cell transplantation, local delivery of the secretome is under investigation to provide the complex signaling milieu for promoting tissue repair [6,13]. There is an urgent need for strategies that potentiate the effect of the secretome to enhance the efficacy of this approach. Compared to monodisperse cells, MSC spheroids exhibit superior viability in harsh microenvironments and increased secretion of bioactive trophic factors, resulting in improved tissue repair [14,15]. While the benefits of MSC transplantation are apparent for musculoskeletal tissue repair, no studies have reported the effect of myokine generated by serial exposure of muscle cells to MSCs on bone regeneration.

We hypothesized that bone formation would be enhanced by local myokine presentation, and the myoblast secretome would be augmented by exposure to factors secreted by MSC spheroids. Our aims were three-fold: (1) evaluate the potential of myokines to stimulate osteogenic differentiation of osteoprogenitor cells, (2) identify key bioactive cues involved in stimulating osteogenesis, and (3) translate this strategic approach to promote bone healing by locally delivering the myoblast secretome to a rat femoral segmental defect model.

2. Materials and methods

2.1. Cell culture

Human bone marrow-derived MSCs from a single donor were purchased from RoosterBio (Frederick, MD). Cells were expanded in α-MEM (Invitrogen, Carlsbad, CA) supplemented with 10% v/v fetal bovine serum (FBS, JR Scientific, Woodland, CA), 100 units/mL penicillin, and 100 μg/mL streptomycin (Gemini Bio-Products, Sacramento, CA) under standard culture conditions until use at passage 4-5. MC3T3-E1 pre-osteoblasts (ATCC, Manassas, VA) and rat bone marrow stromal cells (rBMSCs) (Cyagen Biosciences Inc., Santa Clara, CA) were cultured in similar conditions. L6 rat myoblasts (ATCC) were maintained in DMEM supplemented with 10% v/v FBS, 100 units/mL penicillin, and 100 μg/mL streptomycin under standard culture conditions. Myoblasts were kept below 70% confluency to prevent differentiation and myofibril formation.

2.2. Fabrication of MSC spheroids, conditioning, and media collection

MSC spheroids of 5000 (5 K); 15,000 (15 K); and 40,000 cells/spheroid (40 K) were formed using a forced aggregation technique [15,16]. Media was exchanged with serum-containing fresh media supplemented with 100 mM $CoCl_2$ (Sigma, St. Louis, MO) and maintained for 3 days. Since hypoxia plays a key role in MSC survival, differentiation, and trophic factor secretion, we screened the response of MSCs using two different methods to generate a hypoxic environment: 1) incubation in reduced oxygen (1%) or 2) supplementation of media with the hypoxia mimetic, $CoCl_2$. Spheroids in standard culture conditions and monolayer cultured MSCs served as controls. Spheroids were then washed with PBS, and media was replaced with fresh serum-containing α-MEM for culture in ambient conditions for 24 h and designated as spheroid-conditioned media (SPH). MSCs were maintained in monolayer culture and treated identically to generate monolayer-conditioned media (MCM). Conditioned media from L6 myoblasts was termed myoblast-conditioned media (MYO). Finally, monolayer L6 myoblasts were exposed to SPH for 24 h, after which the media was collected and termed spheroid-myoblast-conditioned media (SPH-MYO) (Fig. 1A). For *in vivo* experiments, conditioned media (6 mL) was lyophilized for 48 h until dry for subsequent entrapment in alginate (Fig. 1B). Media was pooled for all *in vitro* and *in vivo* studies.

2.3. Evaluation of conditioned media on viability and function of osteoblastic cells

MC3T3-E1 murine pre-osteoblasts or rBMSCs were plated at 1.0×10^5 cells/cm^2 in serum-containing complete media and allowed to attach for 24 h. Cells were then exposed to a 50:50 mixture of serum-containing osteogenic media (10 mM β-glycerophosphate, 50 μg/mL ascorbate 2-phosphate; both from Sigma) and conditioned media for 3 days. Subsequent media changes were performed every 3 days with serum-containing complete α-MEM. Cell survival and apoptosis was measured using a Caspase-Glo 3/7 assay (Promega, Madison, WI). Cell metabolic activity was quantified using a Thiazolyl Blue tetrazolium bromide (MTT) assay (Sigma). The osteogenic response of MC3T3-E1s and rBMSCs to conditioned media was assessed by quantifying cell number using a Countess II automatic cell counter (Thermo Fisher, Waltham, MA), DNA content using a PicoGreen DNA assay (Invitrogen), intracellular alkaline phosphatase (ALP) activity from a *p*-nitrophenyl phosphate assay, and calcium deposition by *o*- cresolphthalein assay and Alizarin red staining [17,18]. We identified and evaluated the concentration of growth factors and cytokines within conditioned media using a protein array (Ray Biotech, Norcross, GA) [14].

2.4. Preparation and characterization of RGD-modified alginate

RGD-modified alginate was prepared as described previously [15,19]. Briefly, G_4RGDSP (Commonwealth Biotechnologies, Richmond, VA) was covalently coupled to UltraPure VLVG sodium alginate and 1% oxidized UltraPure MVG (Pronova, Lysaker, Norway) using standard carbodiimide chemistry, yielding hydrogels containing 0.8 mM RGD. The resulting RGD-alginate was sterile filtered and lyophilized for 4 days. Lyophilized alginate was reconstituted in serum-free α-MEM (840 μL) at a 25:75 VLVG:MVG ratio to obtain a 2% (w/v) solution. We then mixed lyophilized SPH-MYO into the alginate, with or without rBMSCs (5×10^6 cells/mL), and gels (60 μL) were cross-linked by dialyzing with 200 mM $CaCl_2$ for 10 min [15].

We measured gel storage modulus using a Discovery HR2 Hybrid Rheometer (TA Instruments, New Castle, DE). An 8.0-mm-diameter Peltier plate geometry was used with an oscillatory strain sweep protocol ranging from 0.004% to 4% strain [20]. We evaluated myokine release from the alginate gels using 2 μg of VEGF (PeproTech, Rocky Hill, NJ) as a model protein. VEGF elution into serum-free media was measured using a VEGF-specific ELISA (R&D Systems, Minneapolis, MN). We confirmed cell viability in gels 3 days after entrapment using a Live/Dead Assay and confocal microscopy.

2.5. Segmental bone defect model

Treatment of experimental animals was in accordance with the UC Davis animal care guidelines and all National Institutes of Health animal handling procedures. SPH-MYO, with or without rBMSCs (30×10^6 cells/mL), was entrapped in alginate hydrogels (60 μL, 3 mm height, 3 mm width, 6 mm length) and kept in complete media in standard culture conditions for 18 h before implantation. We implanted rBMSCs to assess whether myokines and stromal cells could work synergistically to regenerate bone and avoid immunologic reactions to rBMSCs when implanted in immunocompetent rats. Sprague-Dawley rats (male and female, 10 weeks old, Taconic, Hudson, NY) were anesthetized and maintained under a 3–4% isoflurane/O_2 mixture delivered through a nose cone. We created six-millimeter diaphyseal critically sized defects in the right femora of each animal and stabilized these defects with a radiolucent polyetheretherketone (PEEK) plate and 6 angular stable bicortical titanium screws (RISystem AG, Davos, Switzerland) [15,21]. We immediately filled these defects with one of four RGD-modified alginate constructs: 1) acellular gels containing

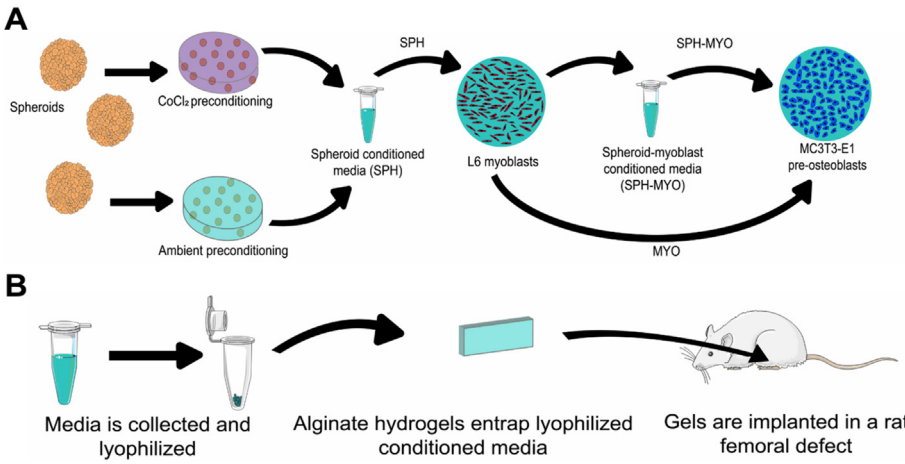

Fig. 1. Schematic of experimental procedure. (**A**) MSC spheroids were preconditioned in either $CoCl_2$ or ambient conditions for 72 h and then maintained in serum-containing growth media for 24 h. Conditioned media was then collected as spheroid-conditioned media (SPH). In some cases, SPH was incubated with L6 myoblasts for 24 h, yielding spheroid-myoblast conditioned media (SPH-MYO). (**B**) Schematic of experiments to investigate the therapeutic potential of conditioned media *in vivo*.

SPH-MYO only; 2) rBMSC-loaded gels; 3) gels containing both SPH-MYO and rBMSCs (SPH-MYO + rBMSCs); or 4) empty gels. Gels were inserted manually using surgical instruments and handled carefully to avoid compression or mechanical stress.

2.6. Quantification of bone formation and assessment of mechanical properties of repair tissue

We monitored bone formation noninvasively using contact high-resolution radiographs (20 kVp, 3 mA, 2 min exposure time, 61 cm source-film distance) taken in a cabinet radiograph unit (Faxitron 43805 N, Field Emission Corporation, Tucson, AZ) with high-resolution mammography film (Oncology Film PPL-2, Kodak, Rochester, NY) and digitized using a high-resolution flatbed scanner. Three blinded, independent reviewers scored these radiographs at 2, 4, 8, and 12 weeks on a scale of 0 (no bone formation) to 6 (homogeneous bone structure). At 12 weeks post-surgery, animals were euthanized, and femurs were explanted, wrapped in sterile gauze, submerged in PBS, and stored at –20 °C until analysis. We imaged explanted femurs (45 kVp, 177 μA, 400 μs integration time, average of four images) at 6 μm resolution using a high-resolution microCT specimen scanner (μCT 35; Scanco Medical, Brüttisellen, Switzerland). Bone volume within the tissue defect and bone mineral density (BMD) were determined from resulting images. We then analyzed explants *via* torsional testing to ascertain mechanical properties of repair tissue [15,21]. Prior to testing, we cut all PEEK plates to ensure stress was concentrated in the defect. The ends of the femurs were potted in Wood's metal and loaded onto the Bose Electroforce 3200 with torsion motor (TA Instruments, New Castle, NE) with an effective testing length of 20 mm. Preloading was performed with ten cycles with a triangle wave to a target rotation of ± 5° at 0.1 Hz. Torsional test to failure was performed such that the femoral head was externally rotated at 1° per second until fracture or complete 90° rotation. Time, position, and torque data were recorded at 50 Hz, and torsional stiffness (N-m degree^{-1}) and ultimate torque (N-m) were calculated. We normalized our data to that of contralateral intact femurs to take into account physiologic differences between rats, adjust for gender-related skeletal differences, and characterize healing progress toward normal bone.

Explants were then demineralized in Calci-Clear Rapid (National Diagnostics, Atlanta, GA), processed, paraffin-embedded, and sectioned at 5 μm thickness. We stained sections with hematoxylin and eosin (H&E) and imaged using a Nikon Eclipse TE2000U microscope and Andor Zyla 5.5 sCMOS digital camera (Concord, MA). We stained tissue sections with Masson's trichrome to visualize collagen deposition within newly formed tissue, while Safranin O/Fast green staining was used to determine if negatively charged substances such as alginate or cartilage were present. Immunohistochemistry for human osteocalcin (1:200, product #AB13420, Abcam), was performed using an HRP detection kit (AB64261, Abcam) per the manufacturer's instructions.

2.7. Statistical analysis

Data are presented as means ± standard deviation. All experiments represent at least three independent experiments unless otherwise noted. Statistical analysis was performed using a one-way analysis of variance with Bonferroni correction for multiple comparisons in Prism 8 software (GraphPad, San Diego, CA); p-values < 0.05 were considered statistically significant. Significance is denoted by alphabetical letterings; groups with no significance are linked by the same letters, while groups with significance do not share the same letters.

3. Results

3.1. Myokines induce pre-osteoblast proliferation and early osteogenic response

We observed an increase in the number of cells when MC3T3-E1 pre-osteoblasts were exposed to MYO *versus* cells maintained in growth media (Fig. 2B). Additionally, MC3T3s treated with MYO for 3 days had greater ALP activity at Day 7 than cells maintained in osteogenic media alone (Fig. 2C). However, calcium deposition at Day 14 was not significantly different between the two groups (Fig. 2D), suggesting that MYO alone lacks sufficient potency to induce long-term osteogenic differentiation.

3.2. MSC spheroids synergistically enhance myokine bioactivity

MSC spheroids exhibited similar viability regardless of cell density (5 K, 15 K, or 40 K) or preconditioning regimen (ambient conditions, $CoCl_2$, or 1% O_2) by live/dead staining (Supplementary Fig. 1A). In preliminary studies, we observed similar osteogenic response of MC3T3-E1 pre-osteoblasts when exposed to preconditioned media from MSCs in $CoCl_2$ or 1% O_2. Due to increased reproducibility of supplementing culture media with small molecules *versus* regulating the local oxygen microenvironment, all subsequent preconditioning was performed using $CoCl_2$. Conditioned media was generated by the same number of MSCs regardless of spheroid density to account for differences in secretome production. Compared to 5 K and 15 K spheroids, conditioned media from 40 K spheroids induced a greater osteogenic response in MC3T3-E1 pre-osteoblasts (Supplementary Fig. 1B–D), motivating the use of 40 K spheroids for all subsequent experiments.

In agreement with previous reports in which MSC spheroids outperform equal numbers of individual MSCs [14], conditioned media from MSC spheroids induced a greater osteogenic response in MC3T3s

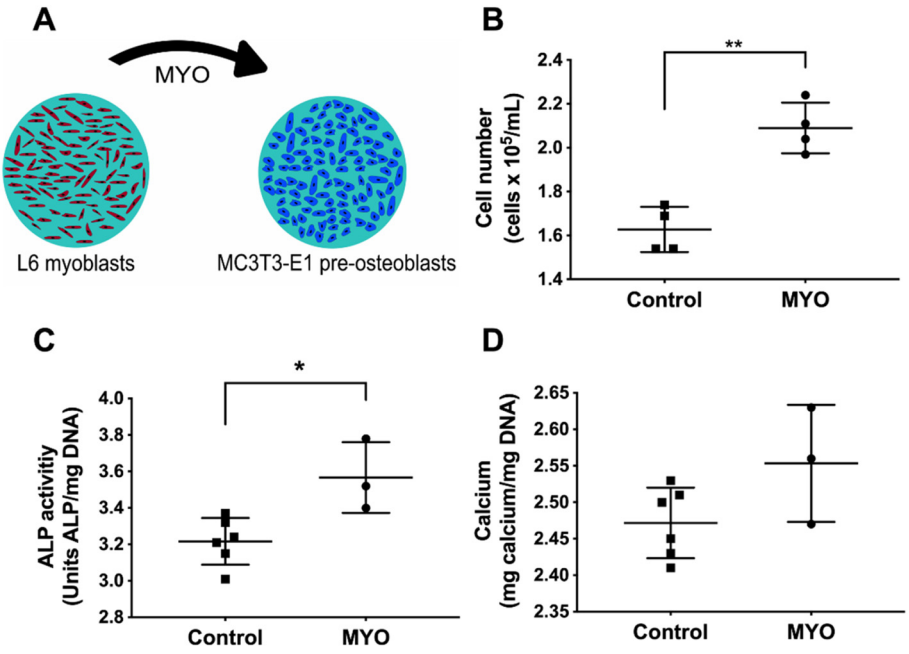

Fig. 2. Myokines induce early osteogenic response in pre-osteoblasts. (**A**) L6 myoblast-conditioned media (MYO) was added to MC3T3-E1 pre-osteoblasts in monolayer culture. (**B**) Cell number at day 3, (**C**) ALP activity at day 7, and (**D**) calcium deposition at day 14 for MC3T3s after exposure to MYO (*$p < 0.05$, **$p < 0.01$; $n = 3$–6). Control groups maintained in osteogenic media alone.

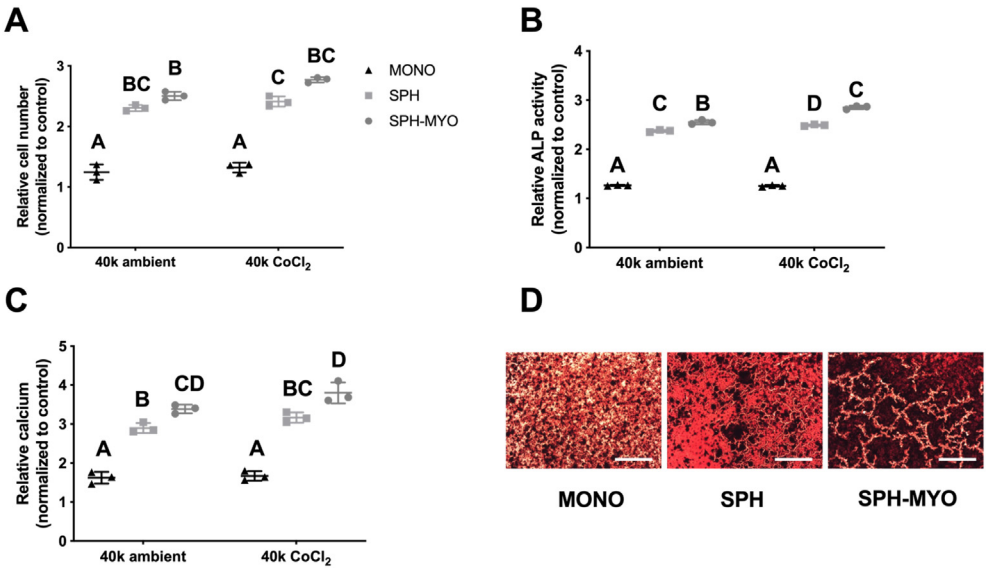

Fig. 3. Investigation of the osteogenic response of conditioned media on pre-osteoblasts. The osteogenic response of spheroid-myoblast conditioned media (SPH-MYO), spheroid conditioned media (SPH) and MSC monolayer-conditioned media (MONO) on MC3T3s was investigated by analyzing (**A**) cell number at day 3, (**B**) ALP activity at day 7, and (**C**) calcium deposition. Data are normalized to the response of MC3T3s in osteogenic media alone ($n = 3$). Data that do not share letters are statistically significant from each other. (**D**) Representative Alizarin red staining of MC3T3s at day 14. Scale bar represents 500 μm. (For interpretation of the references to colour in this figure legend, the reader is referred to the web version of this article.)

compared to MSCs in monolayer culture. We observed significant increases in the number of MC3T3s when exposed to SPH-MYO compared to the SPH and MYO groups (Fig. 3A). We detected similar caspase activity in MC3T3s stimulated with SPH-MYO, MYO, and SPH, but all outperformed the control group by eliciting lower caspase 3/7 activity (Supplementary Fig. 2). MC3T3s exposed to the secretome of MSC spheroids preconditioned in $CoCl_2$ exhibited greater ALP activity, an early marker of osteogenic differentiation, compared to SPH from spheroids in ambient air (Fig. 3B). In the $CoCl_2$ group, ALP activity increased by > 90% in SPH and 120% in SPH-MYO groups compared to MONO ($p < 0.0001$). Calcium deposition, a late-stage functional marker of osteogenic differentiation, was also increased in MC3T3s by 120% when exposed to SPH-MYO compared to MONO ($p < 0.0001$), while SPH induced nearly 90% increase ($p < 0.0001$) (Fig. 3C). SPH-MYO induced significant increases in calcium deposition by MC3T3s (3.39 ± 0.11-fold increase *versus* controls) compared to SPH (2.90 ± 0.13, $p < 0.004$) or MYO (1.03 ± 0.03, $p < 0.001$). We confirmed these quantitative increases in calcium deposition by Alizarin Red staining (Fig. 3D). For both markers, the largest increase in osteogenic markers was induced by exposure to the secretome of MSC spheroids (SPH), and these markers were further increased when exposed to SPH-MYO.

We analyzed the cytokine profiles of each formulation using a protein array to interrogate potential differences in the composition and quantity of cytokines in each secretome (Supplementary Fig. 3). The complexity and quantity of bioactive factors were enhanced in conditioned media from $CoCl_2$-preconditioned spheroids compared to spheroids maintained in ambient conditions. Among the secreted factors examined, we detected appreciable increases in the quantity and complexity of SPH-MYO compared to SPH or MYO alone. We measured nearly a 30% increase IGF-1 and 20% increase in SDF-1α in SPH-MYO compared to SPH, and both factors were increased by > 200%, on average, compared to MYO. Of particular interest, the preconditioned SPH-MYO media contained increased concentrations of IGF-1, IL-8, TIMP1, FGF-6, SDF-1α, and IL-6 compared to SPH and MYO media alone.

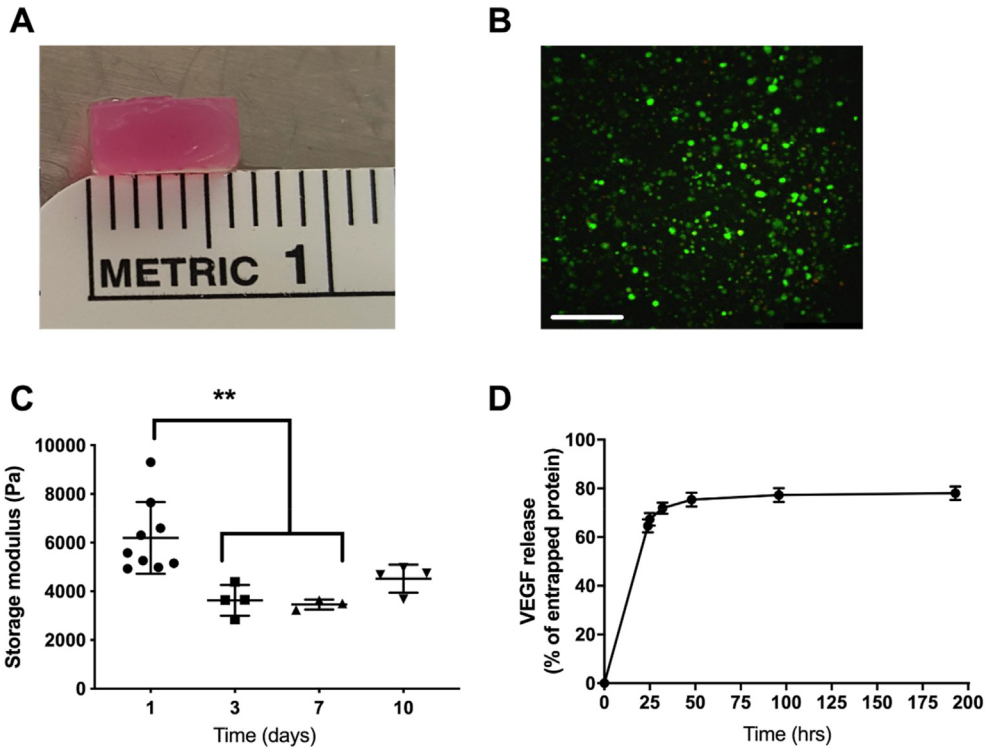

Fig. 4. Characterization of alginate hydrogel properties and delivery of growth factor. (**A**) Macroscopic image of MYO-SPH-loaded alginate hydrogel. (**B**) Live/dead stain of rBMSCs in hydrogel before implantation. Scale bar represents 250 μm. (**C**) Storage modulus of MYO-SPH-loaded hydrogel over 10 days (**D**) Quantification of the release of VEGF as a model protein for entrapped conditioned media. $^{**}p < 0.01$; $n = 3–4$.

3.3. Conditioned media entrapped in alginate hydrogels

Gels were designed and formed to precisely fill surgically created voids when press fit into the femoral defect (Fig. 4A). We observed high viability and homogeneous distribution of entrapped rBMSCs throughout the gel after overnight incubation (Fig. 4B). Similar to results in MC3T3s, we observed increases in osteogenic potential, as measured by calcium deposition, when rBMSCs were exposed to SPH-MYO compared to SPH, MYO, or monolayer-cultured MSCs (MONO) (Supplementary Fig. 4A). When exposed to conditioned media, we observed similar metabolic activity in rBMSCs exposed to SPH or SPH-MYO compared to untreated cells, with MYO inducing a significant increase ($p < 0.05$) in MTT activity (Supplementary Fig. 4B). Upon fabrication, gels could be easily handled and exhibited a decrease in storage modulus after 3 days that remained constant over 10 days (Fig. 4C). The majority of VEGF, serving as a model protein to mimic release of entrapped trophic factors in conditioned media, eluted from the gel over the first 72 h (Fig. 4D).

3.4. Local presentation of myokine-conditioned media increases bone formation in vivo

The local presentation of SPH-MYO from alginate gels, in the presence and absence of rBMSCs, increased bone formation compared to empty hydrogels as measured by blinded radiograph evaluation (Fig. 5A and Supplementary Fig. 5). Importantly, the combined delivery of rBMSCs with SPH-MYO resulted in the greatest bone regeneration among the groups analyzed, which was > 1.6-fold greater than acellular SPH-MYO-containing hydrogels ($p < 0.05$) and > 35-fold greater than rBMSCs alone ($p < 0.0001$). We observed increased bone formation and vascularization within femoral defects treated with SPH-MYO-containing gels by macroscopic tissue images of the defect upon explantation (Fig. 5B). Quantitative measurements of bone volume and bone mineral density using microCT were in agreement with radiography and gross tissue observations, with defects treated with SPH-MYO-containing gels exhibiting the highest bone volume and bone mineral density (Fig. 5C–E). The resultant tissue within bone defects treated with SPH-MYO also possessed the most robust mechanical properties. Femoral defects treated with SPH-MYO-containing gels, particularly those gels also containing rBMSCs, demonstrated the greatest torsional stiffness and torque to failure (Fig. 6A–B), which was 1.5 times greater than SPH ($p < 0.0003$) and 11 times greater than rBMSCs alone ($p < 0.0001$). H&E staining revealed higher cell density in the groups without rBMSCs, while defects treated with rBMSCs contained more organized, dense tissue (Fig. 7A). Masson's trichrome staining of repair tissue confirmed bony tissue formation within the femoral defect with integration with native bone ends. Intense Masson's trichome staining in defects treated with SPH-MYO + rBMSCs indicated robust collagen deposition, while porous pink regions revealed the formation of marrow spaces (Fig. 7B). Safranin O/Fast green staining (Fig. 7C) indicated the presence of negatively charged material through red staining in the empty and SPH-MYO group, potentially corresponding to residual alginate or neocartilage. Bone defects treated with SPH-MYO + rBMSCs exhibited red staining on the outer layer of the blue-stained regenerated bone.

Osteocalcin IHC further confirmed these data, revealing darker staining in the groups containing rBMSCs and indicating bone formation was occurring (Fig. 7D).

4. Discussion

Fractures with local muscle tissue damage and loss represent a clinically devastating but unstudied challenge for tissue regeneration techniques. Frequently, fracture healing in this setting is insufficient, demonstrating the importance of muscle-bone crosstalk in bone repair [22]. Autologous vascularized muscle flap transplantation, the current standard of treatment, increases the rate of fracture healing but has several limitations including restricted donor site availability, significant donor site morbidity, decreased function of donor and recipient sites, complex and specialized secondary surgeries, and a high rate of complications including complete failure of the graft. This study demonstrated the promise of delivering myokines from engineered biomaterials as a potent bioactive cue to upregulate osteogenic differentiation and support the function of transplanted stromal cells in bone

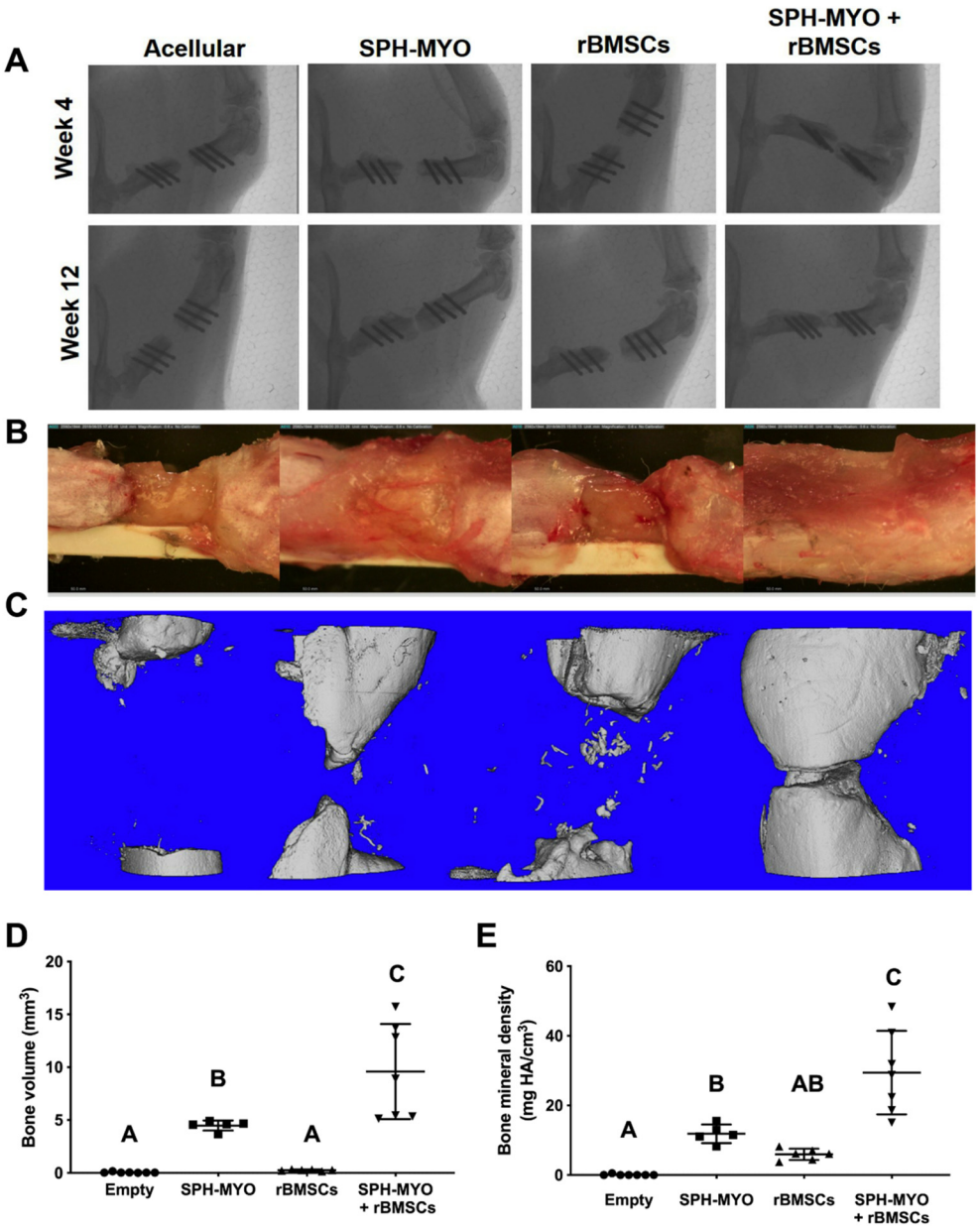

Fig. 5. Repair of rat femoral defect when treated with conditioned media. (**A**) Week 4 and 12 X-rays of the defect. (**B**) Images of explanted femurs at week 12. (**C**) MicroCT images of bone mineralization at week 12 and quantitative microCT data for (**D**) bone volume and (**E**) bone mineral density. Bars that do not share letters are statistically significant from each other (n = 5–7).

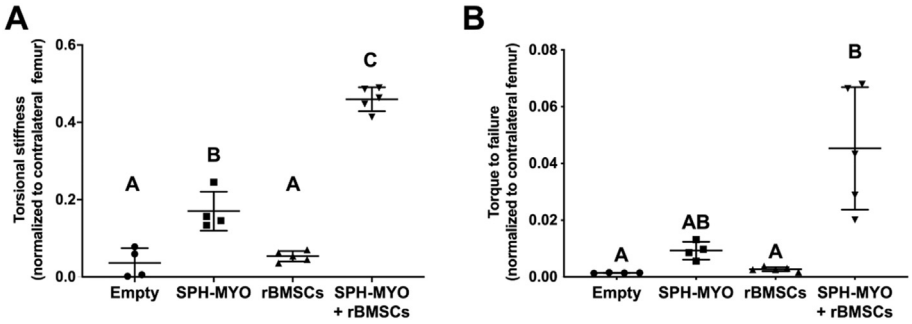

Fig. 6. Mechanical testing of explanted femurs at week 12. Measurement of (**A**) torsional stiffness and (**B**) torque to failure on explanted femurs. Data are normalized to the contralateral femur. Bars that do not share letters are statistically significant from each other (n = 4–5).

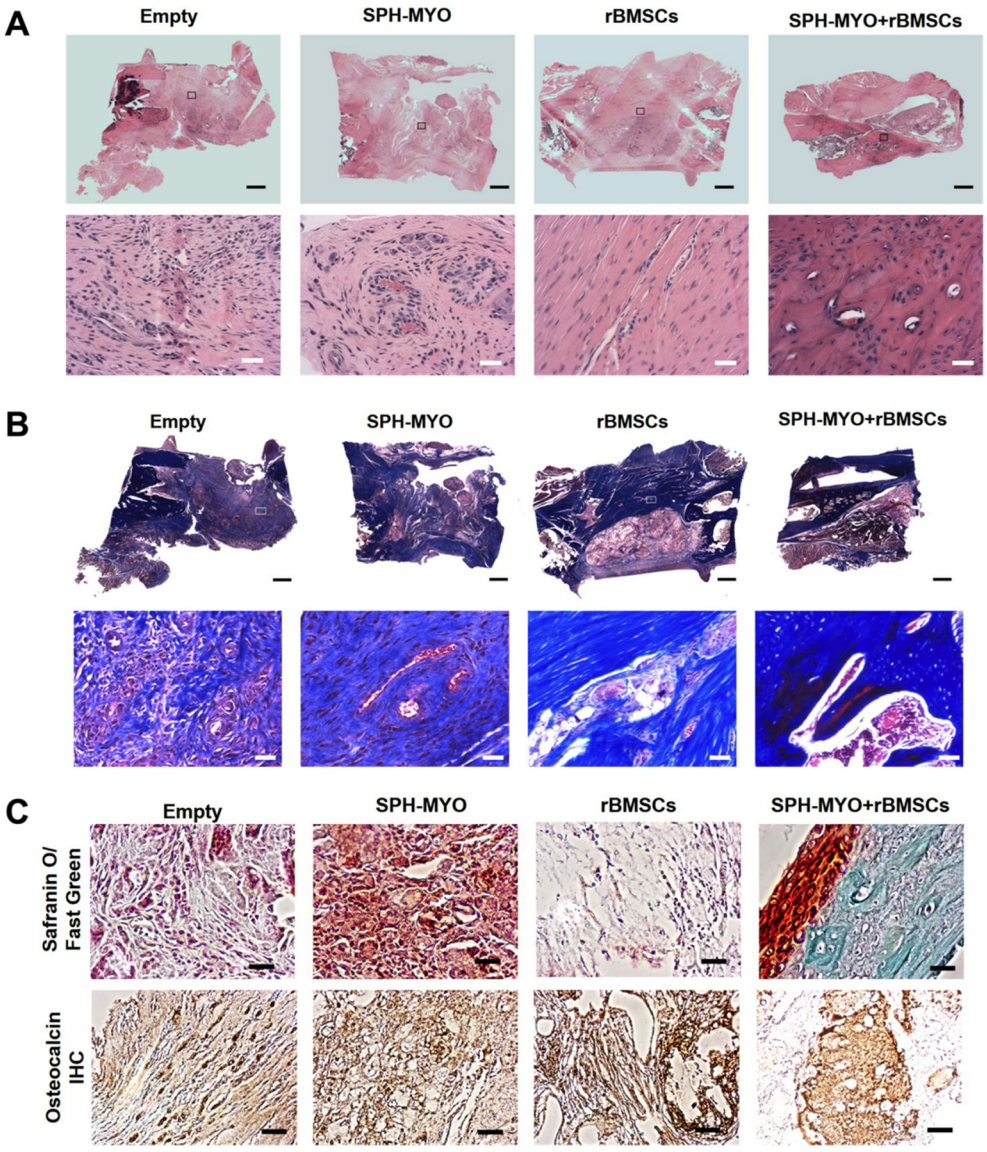

Fig. 7. Histological analysis of regenerated bone tissue. (**A**) Hematoxylin and Eosin (H& E) staining of tissue at the defect site reveals more dense, organized tissue in defects treated with SPH-MYO + rBMSCs. Top images are the entire section, while images below are insets at 20× magnification. (**B**) Masson's Trichrome staining with large scan on top and inset images below at 20× magnification reveals more intense collagen staining in SPH-MYO + rBMSCs compared to other groups. (**C**) 20× magnification images of Safranin O/Fast Green- and osteocalcin-stained sections. Scale bar in large scan is 1 mm; scale bar in 20× images is 50 μm. (For interpretation of the references to colour in this figure legend, the reader is referred to the web version of this article.)

repair. To our knowledge, this is the first demonstration of the synergistic interaction between the paracrine milieu of the MSC spheroid and the myoblast secretome. The translational clinical potential of this therapy is extremely high, as the growth factors are non-immunogenic and possess a prolonged shelf-life when stored as a lyophilized powder [23].

Effective bone repair is reliant on healthy musculature. Fractures involving damaged muscle rarely exhibit bridging compared to fractures in which the muscle remains intact, even with BMP-2 delivery to the defect site [2]. This observation has led to investigation of crosstalk between the two tissues. Muscle enables mechanical loading of the skeleton, which is key to provide sufficient nutrients and induce differentiation of bone cells through fluid flow [7]. The focus of this study was aimed at the endocrine activity of muscle as opposed to its mechanical loading contributions. Although there are over 200 cytokines in the muscle secretome that are implicated in bone repair including IGF-1, BMPs, various interleukins, and others [7], there are few studies that describe their direct therapeutic potency on bone formation. This study confirms the potency of these myokines by identifying them in the conditioned media of myoblasts and MSC spheroids. Myoblasts were used as individual cells that were not fused into myotubes to produce myoblast-conditioned media (MYO), as more mature myofibers secrete growth factors such as ciliary neurotrophic factor (CNTF) that may impair osteogenesis [24]. Each of our groups contained similar concentrations of CNTF, suggesting that other myokines compensated for any downregulation of osteogenesis by this factor.

MSC spheroids possess an enhanced secretome compared to MSCs in monolayer culture, which aids in osteogenesis, modulation of inflammation, and cell engraftment and survival [14,25–27]. Data from these *in vitro* studies are in agreement with previous work, as conditioned media from spheroids (SPH) induced greater cell proliferation, ALP activity, and calcium deposition compared to MONO. We further investigated the potency of this secretome alongside myoblast conditioned media (MYO) and found that calcium production was significantly increased compared to the MYO group. Furthermore, the number and relative concentrations of myokines was greater in SPH compared to MONO and MYO. Spheroid therapeutic potential can be influenced by cell density and pre-conditioning, as spheroids with higher cell density and maintained under hypoxic, pro-inflammatory conditions secrete more VEGF and prostaglandin E2 (PGE_2) [25]. PGE_2 is a critical factor for muscle repair [28], and our previous work demonstrates that PGE_2 secretion is upregulated by MSC spheroids that promote migration of host cells and catalyze bone healing [25,28]. We further demonstrated that the secretome from $CoCl_2$-preconditioned MSC spheroids induced a greater osteogenic response from MC3T3s and rBMSCs compared to spheroids in ambient conditions. The bioactive

nature of the secretome produced by MSCs was similar when stimulated in $CoCl_2$ or 1% O_2. Thus, we focused on $CoCl_2$ conditioning since media supplementation represents an opportunity for greater clinical translation compared to specialized oxygen-controlled incubators. Hypoxic preconditioning of MSCs, whether as monolayer cells or spheroids, results in prolonged viability [29] and increased VEGF secretion [15], demonstrating the value of preconditioning to influence cell function.

Although the MSC spheroid secretome has high therapeutic value, the paracrine activity of muscle for bone repair should not be underestimated. Myoblasts exposed to MSC spheroid-conditioned media produced an enriched conditioned media containing cytokines, myokines, and trophic factors, resulting in increased osteogenic differentiation *in vitro* for bone marrow-derived stem cells and pre-osteoblasts, as well as enhanced bone growth *in vivo*. The cytokine portfolio was more complex than that of MSC spheroids or myoblasts alone, thereby demonstrating a synergistic and augmented relationship. IGF-1 and FGF-2 are potent myokines that promote bone repair [30], and we detected more than a 2-fold increase, on average, of IGF-1 in MYO-SPH compared to MYO or SPH alone. In these studies, we stimulated rat myoblasts with conditioned media from human MSC spheroids, and it is unclear if similar therapeutic benefit would be observed using cells from the same species. However, human recombinant growth factors are highly effective when used in preclinical animal models, and the genetic structure of growth factors such as IGF-1 is well-conserved among mammalian species [31].

To leverage the enhanced osteogenic potential of myokines from serially-stimulated myoblasts, we entrapped conditioned media from SPH-stimulated myoblasts in alginate gels for local presentation at the defect site. Alginate is commonly used as a carrier for cells and macromolecules in tissue regeneration [12,15,32]. While the conditioned media of MSCs has been used to treat other tissues [13,33], this is the first report of efficacy from conditioned media from serially-stimulated cells. Conditioned media was lyophilized for efficient entrapment in small volumes with no apparent adverse effects on growth factor bioactivity or gel stability. We characterized growth factor elution from these alginate hydrogels using VEGF as model protein due to its presence at high concentrations in the MSC secretome and key role in neovascularization. Published studies report similar release kinetics of growth factors from alginate in the presence or absence of cells [34], as alginate is not degraded by mammalian cells like other matrices such as fibrin or collagen. The therapeutic effect of this approach may even be understated considering proteins and cytokines are eluted during the incubation period before hydrogel implantation.

We observed increased bone formation in both defects treated with SPH-MYO, even when rBMSCs were not delivered, demonstrating the healing potential of the augmented myokine secretome. Our study evaluated the osteogenic potential of serially-conditioned media and further explored the synergistic effects of rBMSCs with SPH-MYO *versus* acellular gels *in vivo*. Our findings are in agreement with other reports demonstrating that bone marrow-derived MSCs, whether monodisperse or spheroids, are insufficient to repair large bone defects without preconditioning or osteoinductive stimuli [21,35]. Importantly, the synergistic presentation of SPH-MYO with rBMSCs resulted in significant increases in bone volume and near complete bridging in 12 weeks. These data demonstrate that the conditioned media is actively stimulating resident bone cells and transplanted MSCs to promote cell function and resultant bone formation. However, we were unable to determine the specific role of transplanted rBMSCs in this model. The specific mechanism behind the ability of myokines to enhance cell function *in situ* and influence the surrounding microenvironment merits further investigation. Compared to a true muscle defect, our model retained surrounding healthy muscle tissue that was supplemented by delivery of myokines *via* hydrogel implantation. Further studies utilizing preclinical models of muscle loss are warranted, but our model opens the door to the exploration of injuries such as muscle impairment, a less severe injury but likely more common in most orthopaedic trauma. These data represent the first evidence of myokines locally presented from a carrier in promoting significant bone formation, demonstrating translational potential for use in personalized medicine. This approach facilitates the use of donor cells to manufacture a complex cytokine cocktail that may achieve improved results compared to a single recombinant factor.

5. Conclusion

This study demonstrates the therapeutic potential of myokines in bone healing. Specifically, these data reveal the capacity of myokines stimulated by MSC spheroids to induce osteogenic differentiation *in vitro*, stimulate bone healing *in vivo*, and synergistically support bone marrow stromal cells to bridge critical-sized bone defects. These data emphasize the importance of muscle in bone healing, providing evidence that deficient bone healing in the presence of muscle loss may be due to insufficient myokines secreted from surrounding tissues. Strategies that capitalize on the muscle secretome represent a promising approach to speed the treatment of open fractures with volumetric muscle loss or closed fractures that may suffer from slow or impaired healing due to other comorbidities and complications.

Author contributions

AMS: Conception and design, financial support, collection and/or assembly of data, data analysis, validation, and interpretation, manuscript writing, final approval of manuscript.

MGG: Collection and/or assembly of data, data analysis, validation, and interpretation, manuscript writing, final approval of manuscript.

MAL: Conception and design, interpretation, final approval of manuscript.

JKL: Conception and design, financial support, data analysis and interpretation, manuscript writing, final approval of manuscript.

Declaration of Competing Interest

The authors have no conflicts of interest to declare.

Acknowledgements

Research reported in this publication was supported by the National Institute of Dental and Craniofacial Research of the National Institutes of Health under award number R01 DE025475 to JKL. The work was also supported by a grant from the Orthopaedic Trauma Association to AMS. The content is solely the responsibility of the authors and does not necessarily represent the official views of the National Institutes of Health. The funders had no role in the decision to publish, or preparation of the manuscript. The authors acknowledge Tanya Garcia-Nolen for assistance with microcomputed tomography.

Appendix A. Supplementary data

Supplementary data to this article can be found online at https://doi.org/10.1016/j.bone.2019.05.018.

References

[1] C.M. Court-Brown, K.E. Bugler, N.D. Clement, A.D. Duckworth, M.M. McQueen, The epidemiology of open fractures in adults. A 15-year review, Injury 43 (2012) 891–897.

[2] N.J. Willett, M.-T.A. Li, B.A. Uhrig, J.D. Boerckel, N. Huebsch, T.L. Lundgren, G.L. Warren, R.E. Guldberg, Attenuated human bone morphogenetic protein-2-mediated bone regeneration in a rat model of composite bone and muscle injury, Tissue Eng. Part C. Methods. 19 (2013) 316–325.

[3] Y. Hao, Y. Ma, X. Wang, F. Jin, S. Ge, Short-term muscle atrophy caused by botulinum toxin-A local injection impairs fracture healing in the rat femur, J. Orthop. Res. 30 (2012) 574–580.

[4] M.J. Bosse, E.J. MacKenzie, J.F. Kellam, A.R. Burgess, L.X. Webb,

M.F. Swiontkowski, R.W. Sanders, A.L. Jones, M.P. McAndrew, B.M. Patterson, M.L. McCarthy, T.G. Travison, R.C. Castillo, An analysis of outcomes of reconstruction or amputation after leg-threatening injuries, N. Engl. J. Med. 347 (2002) 1924–1931.
[5] M.D. Helgeson, B.K. Potter, T.C. Burns, R.A. Hayda, D.A. Gajewski, Risk factors for and results of late or delayed amputation following combat-related extremity injuries, Orthopedics 33 (2010) 669.
[6] R.M. Samsonraj, M. Raghunath, V. Nurcombe, J.H. Hui, A.J. van Wijnen, S.M. Cool, Concise review: multifaceted characterization of human mesenchymal stem cells for use in regenerative medicine, Stem Cells Transl. Med. 6 (2017) 2173–2185.
[7] M. Brotto, L. Bonewald, Bone and muscle: interactions beyond mechanical, Bone 80 (2015) 109–114.
[8] P. Niemeyer, K. Fechner, S. Milz, W. Richter, N.P. Suedkamp, A.T. Mehlhorn, S. Pearce, P. Kasten, Comparison of mesenchymal stem cells from bone marrow and adipose tissue for bone regeneration in a critical size defect of the sheep tibia and the influence of platelet-rich plasma, Biomaterials 31 (2010) 3572–3579.
[9] E.M. Fennema, L.A.H. Tchang, H. Yuan, C.A. van Blitterswijk, I. Martin, A. Scherberich, J. de Boer, Ectopic bone formation by aggregated mesenchymal stem cells from bone marrow and adipose tissue: a comparative study, J. Tissue Eng. Regen. Med. 12 (2018) e150–e158.
[10] A. Gianakos, A. Ni, L. Zambrana, J.G. Kennedy, J.M. Lane, Bone marrow aspirate concentrate in animal long bone healing, J. Orthop. Trauma 30 (2016) 1–9.
[11] S.H. Ranganath, O. Levy, M.S. Inamdar, J.M. Karp, Harnessing the mesenchymal stem cell secretome for the treatment of cardiovascular disease, Cell Stem Cell 10 (2012) 244–258.
[12] M. Pumberger, T.H. Qazi, M.C. Ehrentraut, M. Textor, J. Kueper, G. Stoltenburg-Didinger, T. Winkler, P. von Roth, S. Reinke, C. Borselli, C. Perka, D.J. Mooney, G.N. Duda, S. Geißler, Synthetic niche to modulate regenerative potential of MSCs and enhance skeletal muscle regeneration, Biomaterials 99 (2016) 95–108.
[13] M. Osugi, W. Katagiri, R. Yoshimi, T. Inukai, H. Hibi, M. Ueda, Conditioned media from mesenchymal stem cells enhanced bone regeneration in rat calvarial bone defects, Tissue Eng. Part A. 18 (2012) 1479–1489.
[14] S.S. Ho, K.C. Murphy, B.Y.K. Binder, C.B. Vissers, J.K. Leach, Increased survival and function of mesenchymal stem cell spheroids entrapped in instructive alginate hydrogels, Stem Cells Transl. Med. 5 (2016) 773–781.
[15] S.S. Ho, B.P. Hung, N. Heyrani, M.A. Lee, J.K. Leach, Hypoxic preconditioning of mesenchymal stem cells with subsequent spheroid formation accelerates repair of segmental bone defects, Stem Cells 36 (2018) 1393–1403.
[16] C.E. Vorwald, S.S. Ho, J. Whitehead, J.K. Leach, High-throughput formation of mesenchymal stem cell spheroids and entrapment in alginate hydrogels, Methods Mol. Biol, 2018, pp. 139–149.
[17] A. Bhat, A.I. Hoch, M.L. Decaris, J.K. Leach, Alginate hydrogels containing cell-interactive beads for bone formation, FASEB J. 27 (2013) 4844–4852.
[18] M.L. Decaris, B.Y. Binder, M.A. Soicher, A. Bhat, J.K. Leach, Cell-derived matrix coatings for polymeric scaffolds, Tissue Eng. Part A. 18 (2012) 2148–2157.
[19] B.P. Hung, J.N. Harvestine, A.M. Saiz, T. Gonzalez-Fernandez, D.E. Sahar, M.L. Weiss, J.K. Leach, Defining hydrogel properties to instruct lineage- and cell-specific mesenchymal differentiation, Biomaterials 189 (2019) 1–10.
[20] S.S. Ho, A.T. Keown, B. Addison, J.K. Leach, Cell migration and bone formation from mesenchymal stem cell spheroids in alginate hydrogels are regulated by adhesive ligand density, Biomacromolecules 18 (2017) 4331–4340.
[21] S.S. Ho, N.L. Vollmer, M.I. Refaat, O. Jeon, E. Alsberg, M.A. Lee, J.K. Leach, Bone morphogenetic protein-2 promotes human mesenchymal stem cell survival and resultant bone formation when entrapped in photocrosslinked alginate hydrogels, Adv. Healthc. Mater. 5 (2016) 2501–2509.
[22] L.E. Harry, A. Sandison, E.M. Paleolog, U. Hansen, M.F. Pearse, J. Nanchahal, Comparison of the healing of open tibial fractures covered with either muscle or fasciocutaneous tissue in a murine model, J. Orthop. Res. 26 (2008) 1238–1244.
[23] J.F. Carpenter, M.J. Pikal, B.S. Chang, T.W. Randolph, Rational design of stable lyophilized protein formulations: some practical advice, Pharm. Res. 14 (1997) 969–975.
[24] R.W. Johnson, J.D. White, E.C. Walker, T.J. Martin, N.A. Sims, Myokines (muscle-derived cytokines and chemokines) including ciliary neurotrophic factor (CNTF) inhibit osteoblast differentiation, Bone 64 (2014) 47–56.
[25] K.C. Murphy, J. Whitehead, P.C. Falahee, D. Zhou, S.I. Simon, J.K. Leach, Multifactorial experimental design to optimize the anti-inflammatory and proangiogenic potential of mesenchymal stem cell spheroids, Stem Cells 35 (2017) 1493–1504.
[26] J.H. YlÖstalo, T.J. Bartosh, K. Coble, D.J. Prockop, Human mesenchymal stem/stromal cells cultured as spheroids are self-activated to produce prostaglandin E2 that directs stimulated macrophages into an anti-inflammatory phenotype, Stem Cells 30 (2012) 2283–2296.
[27] M.A. Gionet-Gonzales, J.K. Leach, Engineering principles for guiding spheroid function in the regeneration of bone, cartilage, and skin, Biomed. Mater. 13 (2018) 34109.
[28] A.T.V. Ho, A.R. Palla, M.R. Blake, N.D. Yucel, Y.X. Wang, K.E.G. Magnusson, C.A. Holbrook, P.E. Kraft, S.L. Delp, H.M. Blau, Prostaglandin E2 is essential for efficacious skeletal muscle stem-cell function, augmenting regeneration and strength, Proc. Natl. Acad. Sci. U. S. A. 114 (2017) 6675–6684.
[29] J. Beegle, K. Lakatos, S. Kalomoiris, H. Stewart, R.R. Isseroff, J.A. Nolta, F.A. Fierro, Hypoxic preconditioning of mesenchymal stromal cells induces metabolic changes, enhances survival, and promotes cell retention in vivo, Stem Cells 33 (2015) 1818–1828.
[30] M.W. Hamrick, P.L. McNeil, S.L. Patterson, Role of muscle-derived growth factors in bone formation, J. Musculoskelet. Neuronal Interact. 10 (2010) 64–70 (accessed December 7, 2018).
[31] P. Rotwein, Diversification of the insulin-like growth factor 1 gene in mammals, PLoS One 12 (2017) e0189642.
[32] Y.M. Kolambkar, K.M. Dupont, J.D. Boerckel, N. Huebsch, D.J. Mooney, D.W. Hutmacher, R.E. Guldberg, An alginate-based hybrid system for growth factor delivery in the functional repair of large bone defects, Biomaterials 32 (2011) 65–74.
[33] B. Ritschka, M. Storer, A. Mas, F. Heinzmann, M.C. Ortells, J.P. Morton, O.J. Sansom, L. Zender, W.M. Keyes, The senescence-associated secretory phenotype induces cellular plasticity and tissue regeneration, Genes Dev. 31 (2017) 172–183.
[34] Z. Luo, S. Zhang, J. Pan, R. Shi, H. Liu, Y. Lyu, X. Han, Y. Li, Y. Yang, Z. Xu, Y. Sui, E. Luo, Y. Zhang, S. Wei, Time-responsive osteogenic niche of stem cells: a sequentially triggered, dual-peptide loaded, alginate hybrid system for promoting cell activity and osteo-differentiation, Biomaterials 163 (2018) 25–42.
[35] A.B. Allen, J.A. Zimmermann, O.A. Burnsed, D.C. Yakubovich, H.Y. Stevens, Z. Gazit, T.C. McDevitt, R.E. Guldberg, Environmental manipulation to promote stem cell survival in vivo: use of aggregation, oxygen carrier, and BMP-2 co-delivery strategies, J. Mater. Chem. B 4 (2016) 3594–3607.